Am J Cancer Res 2022;12(10):4825-4839
www.ajcr.us /ISSN:2156-6976/ajcr0142831

Original Article

MDK induces temozolomide resistance in glioblastoma by promoting cancer stem-like properties

Xuehui Yu[1,2*], Zhuan Zhou[1,2*], Siyuan Tang[1], Kun Zhang[1], Xingzhi Peng[1,2], Peijun Zhou[1,2], Mingyu Zhang[3], Liangfang Shen[1], Lifang Yang[1,2]

[1]Department of Oncology, Key Laboratory of Carcinogenesis and Cancer Invasion of Ministry of Education, Xiangya Hospital, Central South University, Changsha, Hunan, China; National Clinical Research Center for Geriatric Disorders, Xiangya Hospital, Central South University, Changsha, Hunan, China; [2]Cancer Research Institute, School of Basic Medicine Science, Central South University, Changsha, Hunan, China; [3]Department of Neurosurgery, Xiangya Hospital, Central South University, Changsha, Hunan, China. [*]Equal contributors.

Received March 12, 2022; Accepted August 15, 2022; Epub October 15, 2022; Published October 30, 2022

Abstract: Glioblastoma (GBM) is the most frequently observed and aggressive type of high-grade malignant glioma. Temozolomide (TMZ) is the primary agent for GBM treatment. However, TMZ resistance remains a major challenge. In this study, we report that MDK is overexpressed in GBM, which leads to enhanced proliferation, apoptosis inhibition, increased invasion and TMZ resistance in GBM cells. It was also determined that MDK could significantly improve the stem-like properties of GBM cells. Mechanistically, MDK enhanced p-JNK through Notch1 and subsequently increased the expression of stemness markers, such as CD133 and Nanog, thereby promoting TMZ resistance. Finally, xenograft experiments and clinical sample analysis also demonstrated that MDK knockdown could significantly inhibit tumor growth *in vivo*, and the expression of MDK was positively correlated with Notch1, p-JNK and CD133. This study revealed that MDK induces TMZ resistance by improving the stem-like properties of GBM by upregulating the Notch1/p-JNK signaling pathway, which provides a possible target for therapeutic intervention of GBM, especially in TMZ-resistant GBM with high MDK expression.

Keywords: MDK, stem-like properties, Notch1/p-JNK, temozolomide resistance, glioblastoma

Introduction

Glioma is a common primary infiltrating brain tumor of the central nervous system, with malignancy grades varying from I to IV and histological subtypes. According to the 2016 WHO classification, grades I-II are low-grade gliomas, and grades III-IV are high-grade gliomas. Most high-grade tumors are associated with high malignancy, strong resistance to chemoradiotherapy and worse prognosis [1]. The median overall survival of patients with grade IV glioblastoma (GBM) is approximately 16-18 months, and the 5-year relative survival is less than 10%. Clinically, the high recurrence rate and resistance to chemoradiotherapy have become major therapeutic difficulties in GBM [2]. Therefore, it is of significance to explore the mechanism of therapeutic resistance to improve the efficacy of GBM therapy.

The current standard therapy consists of surgery followed by temozolomide (TMZ) and radiation. Although TMZ combined with radiotherapy can extend patient postoperative survival compared with radiotherapy alone, due to the increase in dose and time in the treatment of GBM, most cases eventually demonstrate resistance to TMZ [3]. Studies have shown that a variety of mechanisms are involved in the regulation of TMZ resistance in GBM, among which the tumor stemness is an important mechanism [4]. Tumor stemness refers to the characteristics of stem cells, such as self-renewal and multi-differentiation potential, which are not only the key driving factors underlying the occurrence, development, recurrence and metastasis of tumors but also represent an important reason for the resistance of tumors to chemoradiotherapy [5, 6]. In recent years, several studies have found that stemness enhancement is

a critical mechanism facilitating of TMZ resistance in GBM. For example, angiopoietin-like 4 protein (ANGPTL4) induces stemness through the EGFR/AKT/4E-BP1 cascade, resulting in TMZ resistance in GBM [7]. Heat shock factor 1 (HSF1) promotes the expression of the stemness marker SOX2 and cancer stem-like properties, such as colony-forming activity, further increasing TMZ resistance in glioma [8]. The miR-381-NEFL axis is important for TMZ resistance in GBM by promoting various multidrug resistance factors and stemness factors [9]. Therefore, exploration of tumor stemness and the underlying regulatory mechanism may provide us with new points of interference and promising targets for TMZ resistance in GBM.

Midkine (MDK) is a heparin-binding growth factor that is involved in a variety of physiological processes. The overexpression of MDK in neuroblastoma, nasopharyngeal carcinoma and other tumor tissues was observed, and it promoted the growth, migration and angiogenesis of tumor cells [10, 11]. Studies have shown that MDK can promote multidrug resistance in lymphoma, gastric cancer and other tumors [12, 13]. In addition, recent studies have found that MDK protein was enriched in spheres of GBM, suggesting that MDK may be involved in the stemness regulation of GBM [14, 15]. Due to the significant differences in the clinical treatment effect between patients with high- and low-grade gliomas, the analysis of differentially expressed molecules with important functions in gliomas of different grades may provide new targets for the diagnosis and intervention of GBM. In the present study, MDK overexpression in GBM was screened out, and further studies on its role and the molecular mechanism of TMZ resistance were explored.

Materials and methods

Reagents

MDK recombinant protein (rhMDK, D620984) was purchased from Sangon (Shanghai, China). SP600125 (HY-12041) is a broad-spectrum JNK inhibitor [16]. Anisomycin (HY-18982) is an antibiotic that can obviously activate JNK [17]. MK-0752 (HY-10974) is a moderately effective γ-secretase inhibitor that inhibits Notch1 by reducing the production of Aβ40 [18]. Valproic acid (HY-10585) is a selective inhibitor of HDAC and activates the Notch pathway [19]. Napabucasin (HY-13919) is a kind of tumor stemness inhibitor [20], and TMZ (HY-17364) was purchased from MedChemExpress (Monmouth Junction, NJ, USA).

Clinical samples and transcriptome sequencing

Ten surgical tissue samples of gliomas, including 5 cases of grade IV GBM and 5 cases of grade II gliomas (Table S1), were obtained from Xiangya Hospital of Central South University. It was approved by the Ethics Committee of Xiangya Hospital, and all patients signed an informed consent form. The samples were analyzed at the transcriptome level by RNA sequencing at Novogene (Beijing, China).

Cell cultures and transfection

HS683 (ATCC HTB-138) cells were cultured in RPMI-1640 medium (Gibco BRL, Gaithersburg, MD, USA) supplemented with 10% fetal bovine serum (FBS, HyClone, Logan, UT, USA). HEK 293T (ATCC® CRL-11268) and three GBM cell lines, T98G (CRL-1690), LN229 (CRL-2611) and U251, were cultured in DMEM (Gibco BRL) supplemented with 10% FBS (HyClone). Cells were incubated at 37°C in a humidified incubator at 5% CO_2. MDK- and control-siRNA were synthesized by Ribo Biotechnology (Guangzhou, China), and the siRNA sequences are listed in Table S2. Lipofectamine™ 3000 (1888676, Invitrogen, Carlsbad, CA, USA) was used to transfer siRNA into cells following the manufacturer's protocol.

To establish the T98G-shMDK and LN229-shMDK cell lines, MDK-specific shRNA was purchased from GenePharma (Shanghai, China) and cloned into the pLVX-shRNA1 vector (632177, Clontech, Mountain View, CA, USA). Sequences of shRNAs are described in Table S3. For recombinant transfection, lentivirus was produced by cotransfecting 293T cells with shRNA plasmid and packaging plasmids (Gag-pol, pRSV-Rev and pCMV-VSV-G, Addgene, 14887, 12253, 8454, respectively). Viral supernatants were harvested after 48 h of transfection and then used to infect T98G and LN229 cells. Cells were stably selected and pooled with puromycin to obtain stable cell lines.

Real-time quantitative PCR (qPCR)

Total RNA was extracted using TRIzol (15-596026, Thermo Fisher Scientific, Waltham, MA, USA) following the manufacturer's protocol. Then, RNA was processed using a reverse-transcription kit (K1621, Thermo Fisher Scientific) according to the manufacturer's instructions. PCR amplification was performed with TaqMan™ Gene Expression Master Mix (4369016, Thermo Fisher Scientific) using an ABI 7500 instrument (Foster City, CA, USA). qPCR primers are listed in Table S4.

Western blot analysis

Cells were lysed using IP lysis buffer with 10% cocktail (B14001, Bimake, Houston, TX, USA) and quantified using a BCA kit (Pierce Chemical, Rockford, IL, USA). Then, proteins were separated using 10% SDS-PAGE gels and transferred onto polyvinylidene fluoride (PVDF) membranes (Merck Millipore, Billerica, MA, USA) using a Trans-Blot Turbo transfer system (Bio-Rad, Hercules, CA, USA) followed by blocking with 5% nonfat dry milk in Tris-buffered saline-Tween 20 (TBST). The PVDF membranes were probed with primary antibodies followed by a secondary antibody and then detected by an enhanced chemiluminescence reaction with luminol substrate solution (Pierce™, Thermo Fisher). Visualization of proteins was performed using the ChemiDoc XRS system (Bio-Rad). Anti-MDK (ab52637), anti-CD133 (ab216323) and anti-p-ALK (phosphor Y1507, ab73996) antibodies were purchased from Abcam (Cambridge, MA). Anti-P38 (8690), anti-p-P38 (thr180/try182,4511), anti-AKT (9272), anti-ERK (4695), anti-p-ERK1/2 (Thr202/Tyr204, 4370), anti-p-STAT3 (Tyr705, 9145T), anti-Nanog (4903), anti-Nestin (33475S) and anti-LC3 (3868S) were purchased from Cell Signaling Technology (Danvers, MA, USA). Anti-STAT3 (10253-2-AP) and anti-p-Akt (Ser473, 66444-1-Ig) were purchased from Proteintech (Chicago, USA). Anti-ALK (sc-398791) and anti-Notch1 (sc-376403) were purchased from Santa Cruz Biotechnology (Dallas, Texas, USA). Anti-p-JNK (Thr183+Tyr185, AF3318) was purchased from Affinity Biosciences (Cincinnati, OH, USA). Anti-JNK (SAB4200176) was purchased from Sigma-Aldrich (St. Louis, MO, USA). Anti-actin (AC026) was purchased from ABclonal (Wuhan, China). Except for anti-ALK (1:500) and anti-Notch1 (1:500), all primary antibodies were diluted 1:1000 for western blotting.

MTS assay

Cell viability and proliferation were measured by an MTS kit (G5421, Promega, Madison, WI, USA). Cells were plated in 96-well plates and incubated for 0, 24, 48, and 72 h. For each time point, 200 μl of MTS mixture was added per well, and cells were incubated in a 37°C incubator for 1.5 h under conditions away from light. A microplate reader (BioTek ELx800, Winooski, VT, USA) was used to calculate the results at 490 nm.

Colony formation assay

Cells were seeded into 6-well plates and cultured for 2-3 weeks. Colonies in dishes were fixed with 4% paraformaldehyde and stained with 0.1% crystal violet for 15 min. The number of colonies with at least 50 cells was counted under a microscope (DMI3000B, Leica, Wetzlar, Germany).

Flow cytometry

Cells were treated and collected, trypsinized and analyzed with an Annexin-V FITC/PI Apoptosis Detection Kit (KGA107, KeyGEN BioTECH, Jiangsu, China) according to the manufacturer's protocols. Apoptotic analysis was performed with a flow cytometer (FlowSight, Millipore, Billerica, MA, USA).

Scratch assay

Cells were seeded in 24-well plates and grown to 90% confluence. Then, a sterile 200 μl pipette tip was used to make a single scratch in the bottom of the well, and cell culture was performed for the appropriate time. Images were captured with a microscope (DMI3000B, Leica).

Transwell assay

A total of 1×10^5 cells were added to the upper chamber (353097, Corning, NY, USA) of a Transwell insert covered with Matrigel (356230, BD Biosciences, San Jose, CA, USA), and the lower chamber contained medium supplemented with 10% FBS and cultured for 48 h. Then, penetrated cells were fixed with 4% paraformal-

dehyde and stained with 0.1% crystal violet for 15 min. The number of invaded cells in each group was counted under a microscope (DMI3000B, Leica).

Sphere formation assay

Cells were seeded into ultralow-attachment 6-well plates (Corning) with serum-free DMEM/F12 medium containing EGF (PeproTech, NJ, USA), basic fibroblast growth factor (bFGF, Sigma-Aldrich), B27 supplement and N-2 Plus Media supplement (Life Technologies, NY, USA). After incubation for 1-2 weeks, cells were counted and photographed under a microscope (DMI3000B, Leica).

Immunofluorescence assay

After the spheres attached to the poly-L-lysine (PLL) slides, they were fixed with 4% paraformaldehyde for 20 min, permeated with 5% Triton 100 for 15 min and blocked with 10% donkey serum for 1 h. The primary antibody was incubated overnight at 4°C. The primary antibodies used were anti-Nestin (1:2000, 33475S, CST), anti-CD133 (1:500, ab216323, Abcam), and anti-Nanog (1:200, 4903, CST). Then, a fluorescent secondary antibody (SAB4600042, anti-mouse or SAB4600234, anti-rabbit, Sigma-Aldrich) was incubated for 45 min at room temperature followed by DAPI staining solution (E607303, BBI Life Sciences, Shanghai, China) to dye the nuclei. To prevent fluorescence quenching, a reagent (E675001, BBI Life Sciences, Shanghai, China) was used to seal slides, and the fluorescence images were captured by a confocal microscope (LSM 510 META, Carl Zeiss, Germany).

In vivo experiments

All animal work was approved by the Animal Ethics Committee of Xiangya Hospital according to the guidelines of the Institutional Animal Care and Use Committee. Twenty female athymic nude mice (BALB/C) used in the present study were randomly divided into 4 groups: LN229, LN229-shMDK, LN229+TMZ and LN229-shMDK+TMZ. A total of 1×10^7 cells were resuspended in 150 μl of PBS and injected into each mouse to establish xenografts. Tumor volume was measured every 3 days after injection of tumor cells. Intraperitoneal injection of TMZ (1 mg/d/20 g, once a day, lasting 4 days, 2 rounds) was performed after the tumor volume reached 60-80 mm^3. The tumor volume was calculated as volume (mm^3) = $d^2\times D/2$, where d and D were the shortest and longest diameters, respectively.

Immunohistochemistry (IHC)

Forty GBM clinical tissues were obtained from Xiangya Hospital of Central South University. The clinical and pathological features of GBM patients are shown in Table S5. Immunohistochemistry was conducted according to the instructions of a two-step immunohistochemistry kit (PV-9000, ZSGB-BIO, Beijing, China) and DAB kit (ZLI-9017, ZSGB-BIO, Beijing, China) with the following specific primary antibodies: anti-MDK (1:50, ab52637, Abcam), anti-Notch1 (1:100, sc-376403, Santa Cruz), anti-p-JNK (1:200, AF3318, Affinity), and anti-CD133 (1:500, ab216323, Abcam). Stained slides were scored according to the intensity of staining (-: 0; +: 1; ++: 2; and +++: 3) and the percentage of cells of interest staining positive for each antigen (0%: 0; 1~25%: 1; 26~50%: 2; 51~75%: 3; and 76~100%: 4). The intensity score was multiplied by the percentage score to obtain a final score, which was used in the statistical analyses [21].

Bioinformatics analysis

The gene expression profiles were from The Cancer Genome Atlas Program (TCGA) and Chinese Glioma Genome Atlas (CGGA), which were also employed to analyze the effect of MDK expression on overall survival among GBM patients.

Statistical analysis

Statistical analyses were performed using SPSS 19.0 statistical software (IBM-SPSS Statistics, Chicago, IL, USA). Statistical differences were determined by Student's t-test and one-way ANOVA, and a p value <0.05 was considered to be significant. The correlations between IHC-determined gene expression levels were evaluated by Kendall's tau correlation tests.

Results

MDK is overexpressed in GBM and negatively correlated with the prognosis of GBM patients

RNA sequencing was performed using 5 clinical specimens of GBM and 5 cases of low-grade

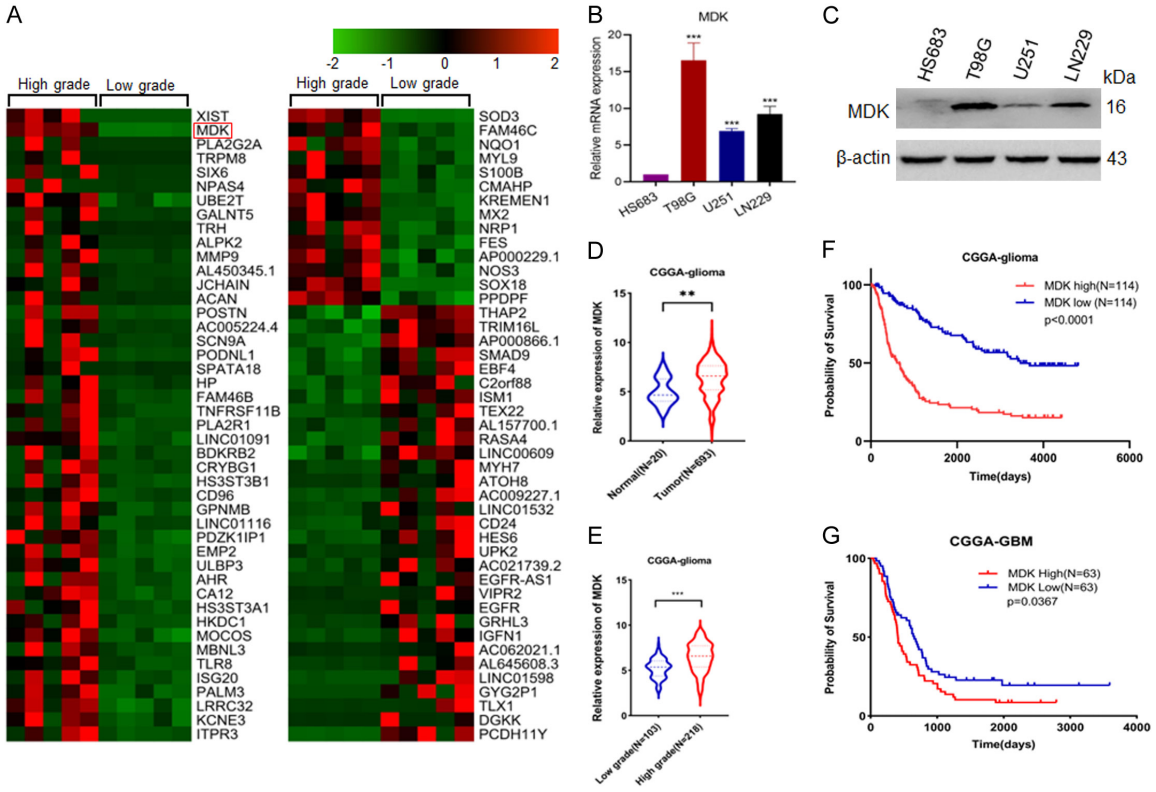

Figure 1. MDK is overexpressed in GBM and negatively correlated with the prognosis of patients. (A) RNA sequencing was used to screen differentially expressed genes in 5 clinical samples of high-grade gliomas and 5 clinical samples of low-grade gliomas. (B) qRT-PCR and (C) western blot analysis of MDK expression in the low-grade glioma cell line HS683 and GBM cell lines T98G, LN229 and U251. (D) The differences in MDK expression between normal glial tissues and glioma tissues were analyzed based on the CGGA database. (E) The differences in MDK expression between low-grade glioma tissues and high-grade glioma tissues were analyzed based on the CGGA database. (F) The correlation between the expression of MDK and the prognosis of glioma patients was analyzed based on the CGGA database. (G) The correlation between the expression of MDK and the prognosis of GBM patients was analyzed based on the CGGA database. Columns: mean of three replicates, **: $p<0.01$, ***: $p<0.001$.

glioma. There were 90 differentially expressed genes in the two groups, 31 of 90 genes were significantly downregulated, and 59 of the 90 genes were significantly upregulated in GBM when the ratio of the genes in GBM to that in low-grade glioma was ≥2 ($p\leq0.05$), among which the expression of MDK was upregulated significantly in GBM (**Figure 1A**). The low-grade glioma cell line HS683 and GBM cell lines T98G, LN229 and U251 were used for verification at the mRNA and protein levels. The results showed that MDK was overexpressed in GBM cells compared with HS683 cells (**Figure 1B** and **1C**). According to CGGA and TCGA database analysis, the expression of MDK in glioma tissue was higher than that in normal tissue (**Figures 1D**, S1A), and its expression was positively correlated with glioma grade (**Figures 1E**, S1B). Moreover, the high expression of MDK in patients with glioma or GBM had a significantly poor prognosis ($p<0.001$) (**Figure 1F** and **1G**). These data suggested that MDK may be involved in the progression of GBM.

MDK promotes proliferation and invasion and inhibits apoptosis in GBM cells

To determine the influence of MDK on GBM cell proliferation, T98G and LN229 cells were transfected with target MDK siRNA, and MTS, colony formation and flow cytometry assays were performed. The results showed that knocking down MDK significantly inhibited cell proliferation ($p<0.001$) (Figures S2, **2A** and **2B**) and promoted cell apoptosis (**Figure 2C**). Furthermore, the results of scratch and Transwell experi-

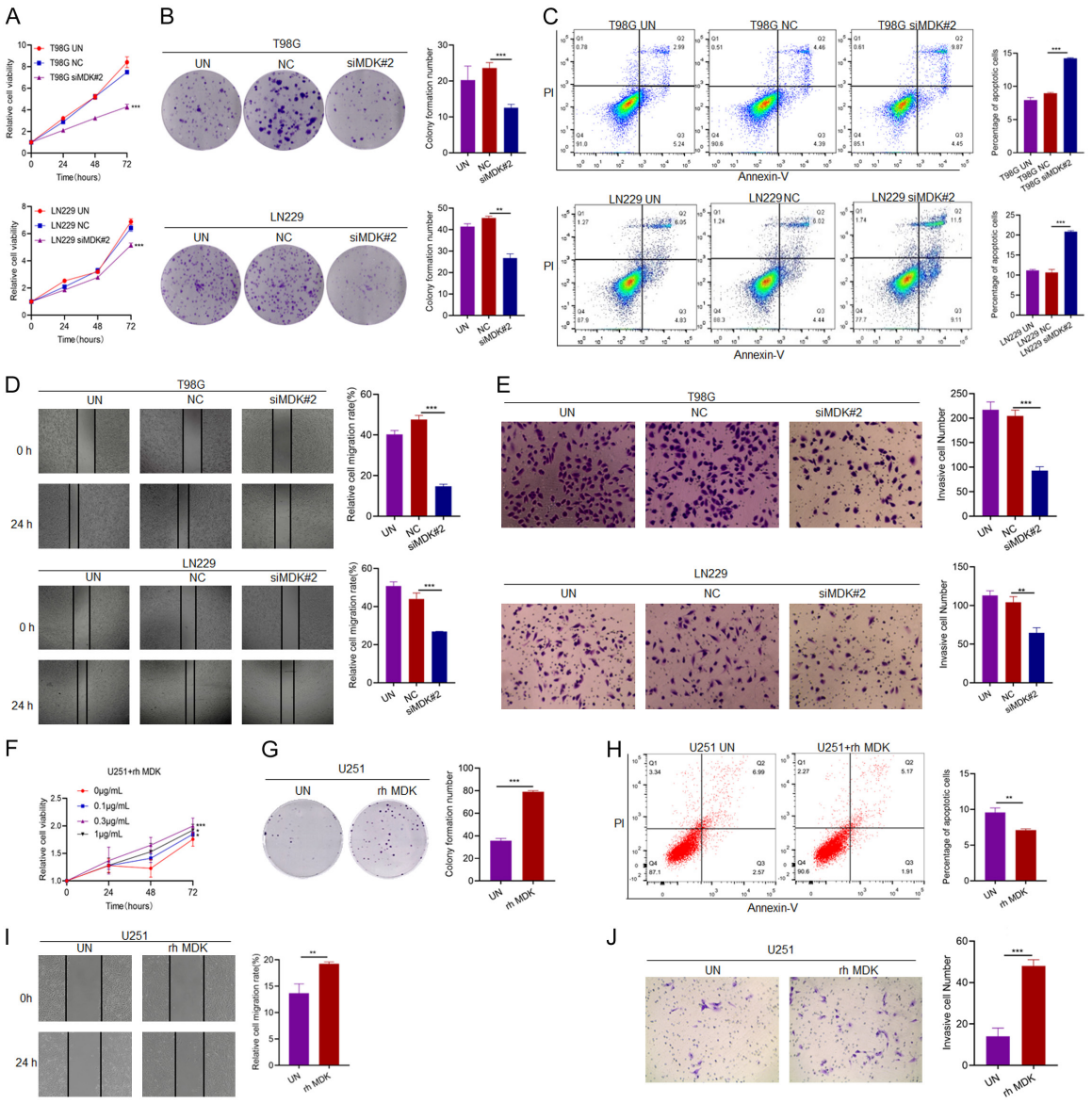

Figure 2. MDK promotes proliferation and invasion and inhibits apoptosis in GBM cells. After transfection of T98G and LN229 cells with siMDK (100 nmol/L) for 24 h, (A) MTS and (B) colony formation assays were used to analyze cell proliferation. (C) Flow cytometric analysis was performed to detect cell apoptosis. (D) Wound healing and (E) Transwell assays were applied to analyze cell migration and invasion. In U251 cells treated with rhMDK (0.3 μg/mL), (F) MTS and (G) colony formation assays were used to analyze cell proliferation. (H) Flow cytometric analysis was performed to detect cell apoptosis. (I) Wound healing and (J) Transwell assays were applied to analyze cell migration and invasion. UN: untreated, NC: negative control. Columns: mean of three replicates, *: $p<0.05$, **: $p<0.01$, ***: $p<0.001$.

ments showed that the migration and invasion ability of GBM cells decreased ($p<0.001$) (**Figure 2D** and **2E**). In U251 cells treated with recombinant human MDK (rhMDK), the data showed that rhMDK promoted cell proliferation ($p<0.001$) (**Figure 2F** and **2G**), inhibited cell apoptosis ($p<0.01$) (**Figure 2H**), and promoted cell migration and invasion ($p<0.01$) (**Figure 2I** and **2J**). These results suggested that MDK participates in the progression of GBM.

MDK induces TMZ resistance in GBM cells

To investigate whether MDK affects TMZ resistance in GBM, first, the IC50 of TMZ on T98G, LN229 and U251 cells was identified (Figure S3). Then, combination treatment with targeted siMDK and TMZ decreased the growth ability of GBM cells more significantly than treatment with TMZ alone ($p<0.001$) (**Figure 3A**), and cell apoptosis increased significantly (**Figure 3B**).

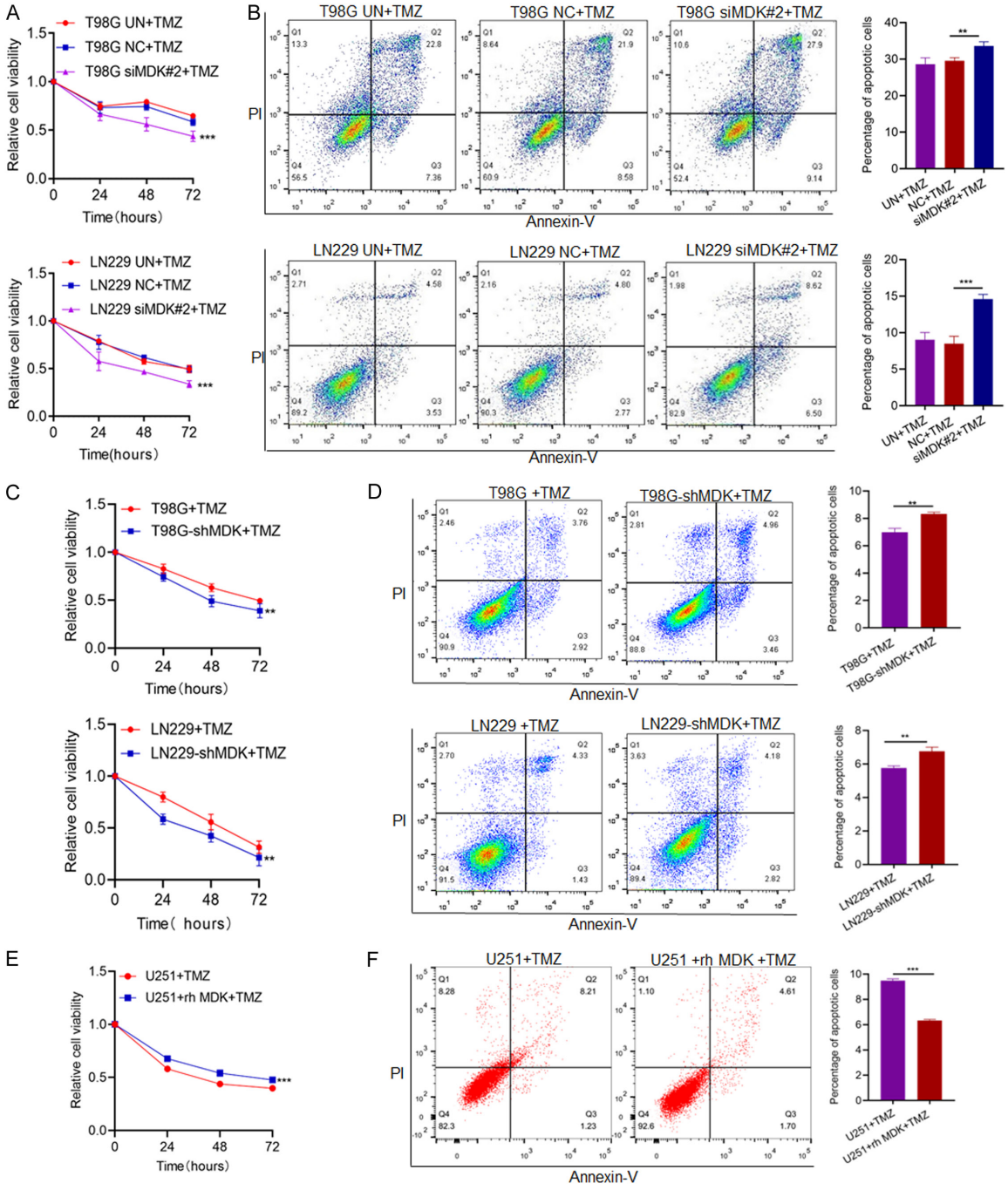

Figure 3. MDK induces TMZ resistance in GBM cells. siMDK was transiently transfected into GBM cell lines T98G and LN229 for 24 h and then treated with TMZ (T98G: 700 μM, LN229: 600 μM). A. The MTS assay was used to analyze cell proliferation. B. Flow cytometric analysis was performed to observe cell apoptosis. T98G-shMDK and LN229-shMDK cells or U251 cells were treated with 0.3 μg/ml rhMDK for 24 h and then treated with TMZ. C and E. MTS assays were used to analyze cell proliferation. D and F. Flow cytometric analysis was performed to observe cell apoptosis. UN: untreated, NC: negative control. **: $p<0.01$, ***: $p<0.001$.

Furthermore, T98G-shMDK and LN229-shMDK cells with stable MDK knockdown were generated (Figure S4). The results of MTS and flow cytometry were consistent with the results of transient knockdown of MDK (**Figure 3C** and **3D**). Moreover, after U251 cells were treated with rhMDK, the data showed that rhMDK could promote cell proliferation, inhibit cell

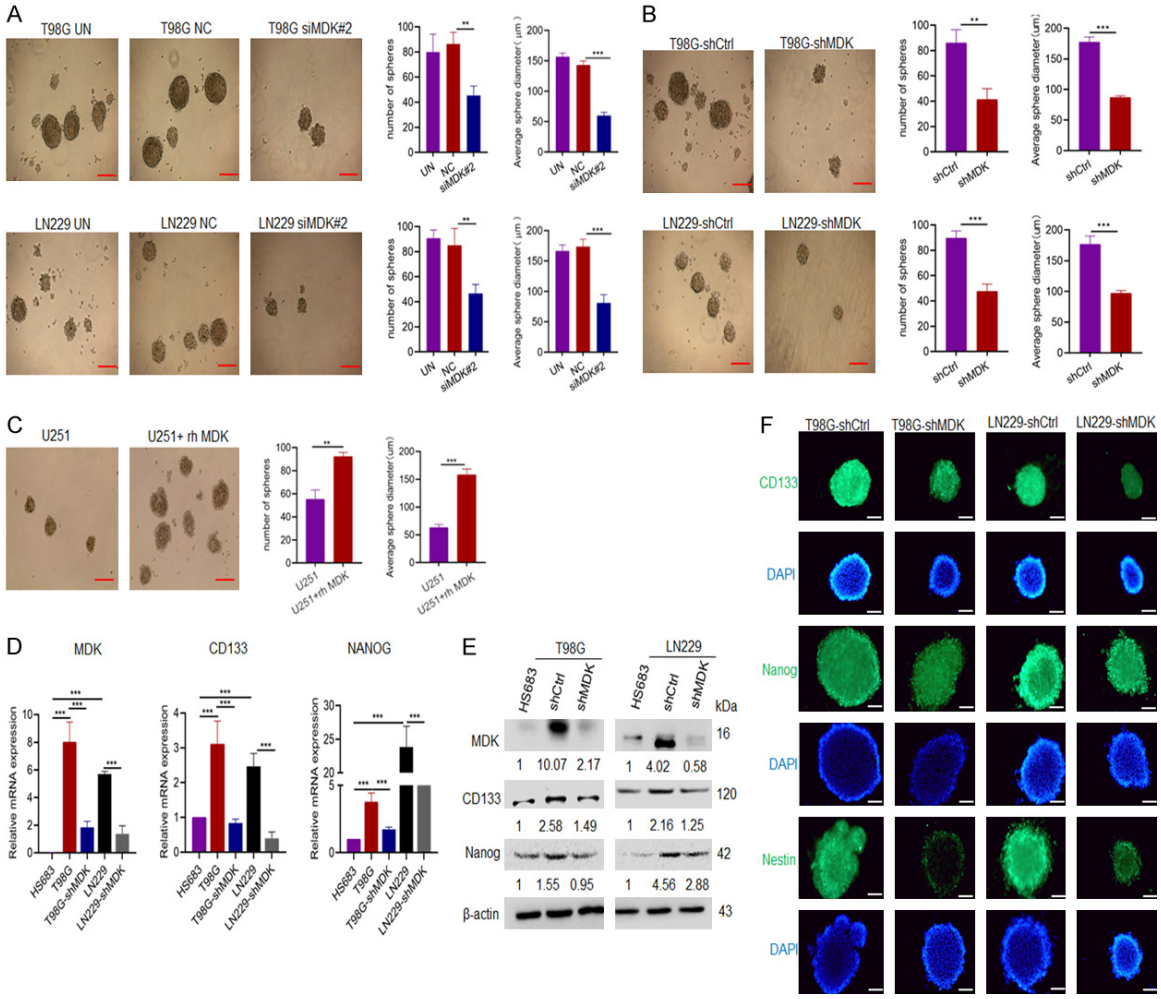

Figure 4. MDK upregulates the stem-like properties of GBM cells. (A) T98G and LN229 cells were transfected with siMDK, (B) T98G-shMDK and LN229-shMDK and (C) U251 cells after rhMDK treatment (0.3 μg/mL), and the sphere formation of cells was detected (2 weeks). (D) qRT-PCR and (E) Western blotting were performed to analyze the expression of MDK and the stemness markers CD133 and Nanog in H683, T98G, T98G-shMDK, LN229 and LN229-shMDK cells. (F) An immunofluorescence assay was performed to observe the expression of CD133, Nanog and Nestin in the spheres of T98G-shMDK and LN229-shMDK cells. Scale bar: 100 μm. UN: untreated, NC: negative control. Columns: mean of three replicates, **: $p<0.01$; ***: $p<0.001$.

apoptosis and reduce the TMZ sensitivity of cells (**Figure 3E** and **3F**). These results showed that MDK can promote TMZ resistance in GBM cells.

MDK upregulates the stem-like properties of GBM cells

Studies have shown that TMZ resistance is mainly related to autophagy, stemness, DNA damage repair and so on [4]. To determine which is involved in MDK-mediated TMZ resistance in GBM cells, the autophagy marker LC3 was detected, and the results showed that there was no significant change in LC3 after knocking down MDK, indicating that TMZ resistance mediated by MDK is not regulated by autophagy (Figure S5). For stem-like properties of GBM cells, the results showed that the size and number of spheres decreased significantly after knocking down MDK in GBM cells ($p<0.01$) (**Figure 4A** and **4B**). Meanwhile, the size and number of spheres increased significantly after rhMDK treatment in U251 cells ($p<0.01$) (**Figure 4C**). Furthermore, the mRNA and protein expression of stemness marker molecules CD133 and Nanog were decreased obviously after knocking down MDK in GBM cells (**Figure 4D** and **4E**), and the immunofluorescence results also showed lower expression of CD133, Nanog and Nestin after knocking down MDK in

GBM cells (**Figure 4F**). These results showed that MDK could promote the stem-like properties of GBM cells.

MDK regulates stem-like properties through the Notch1/p-JNK signaling pathway

Studies have shown that MDK regulates signaling pathways such as ALK, P38, ERK, JNK, AKT, STAT3, and Notch1 to affect multiple functions in tumor cells [11, 15, 22-24]. To clarify which pathway is mainly responsible for MDK regulating stem-like properties of GBM cells, after knocking down MDK, western blotting was performed, and the results showed that the expression of ALK, P38, ERK, AKT, STAT3 and the corresponding phosphorylated proteins did not change obviously in LN229 and T98G cells, while the expression of p-JNK and Notch1 was significantly decreased (**Figure 5A**). Furthermore, the expression of the stemness markers CD133 and Nanog was significantly downregulated, followed by a decrease in p-JNK and Notch1 (**Figure 5B**). Moreover, CD133 and Nanog expression increased with the upregulation of p-JNK and Notch1 after treatment with rhMDK in U251 cells (**Figure 5C**). The results indicated that p-JNK decreased, but Notch1 expression did not change after treatment with the p-JNK inhibitor SP600125, whereas both Notch1 and p-JNK decreased after treatment with the Notch1 inhibitor MK-0752 in GBM cells (Figures S6A and S6C, **5D**). These results suggested that Notch1 could promote p-JNK expression in GBM cells and that the Notch1/p-JNK signaling axis is responsible for MDK-induced stem-like properties in GBM cells.

MDK induces TMZ resistance in GBM cells by promoting cancer stem-like properties

To clarify whether MDK induces TMZ resistance by promoting stem-like properties in GBM cells, the stemness inhibitor napabucasin was used, and the results indicated that it could inhibit the expression of CD133; moreover, MDK expression was not changed in T98G and LN229 cells (Figures S6, **6A**). Napabucasin treatment significantly enhanced TMZ sensitivity according to sphere formation and MTS assay in T98G and LN229 cells (**Figure 6B** and **6C**), suggesting that the stemness of tumor cells was involved in TMZ resistance. Furthermore, a Notch1 inhibitor (MK-0752) and agonist (valproic acid) and a p-JNK inhibitor (SP600125) and agonist (anisomycin) were used. The sphere formation data obtained using the stable knockdown MDK cell lines T98G-shMDK and LN229-shMDK showed that inhibition of Notch1 and p-JNK could decrease sphere forming ability, while activated Notch1 and p-JNK could reverse the effect (Figures S7, **6D** and **6F**). The results of MTS also showed that activating Notch1 and p-JNK could reduce the TMZ sensitivity caused by knocking down MDK (**Figure 6E** and **6G**). After rhMDK treatment in U251 cells, the significant increase of sphere forming ability and cell viability was observed. However, the inhibition of Notch1 and p-JNK by MK-0752 and SP600125 (their action concentrations were determined according to previous studies [16, 18]), can reverse the effect (**Figure 6H** and **6I**), implying that inhibiting Notch1 and p-JNK could suppress the TMZ resistance caused by overexpression of MDK. These results suggested that MDK induced TMZ resistance by promoting the stem-like properties of GBM cells through the Notch1/p-JNK pathway.

MDK knockdown suppresses GBM growth through the Notch1/p-JNK pathway

To investigate whether MDK induces TMZ resistance and promotes GBM growth *in vivo*, a xenograft experiment was performed using LN229-shCtrl and LN229-shMDK cells. As shown in **Figure 7**, TMZ significantly inhibited the growth of tumors, and there was no tumor growth after MDK knockdown (**Figure 7A-C**). Furthermore, IHC staining of forty clinical GBM samples showed obvious decreases in MDK, Notch1, p-JNK and CD133 expression in low-grade tissues compared to high-grade tissues (**Figure 7D** and **7E**), and the correlation analysis implied a positive correlation between MDK, Notch1, p-JNK and CD133 (**Figure 7F**). These results further indicated that MDK promotes stem-like properties through the Notch1/p-JNK pathway, which leads to tumor growth in GBM.

Discussion

Several reports have shown that MDK induces drug resistance in some tumors. Overexpression of MDK could increase the resistance of chemotherapeutic agents (5-FU, doxorubicin, and cisplatin) in cervical carcinoma and gastric cancer cells [13]. MDK induces EMT by increasing the Notch1 signaling pathway and promotes

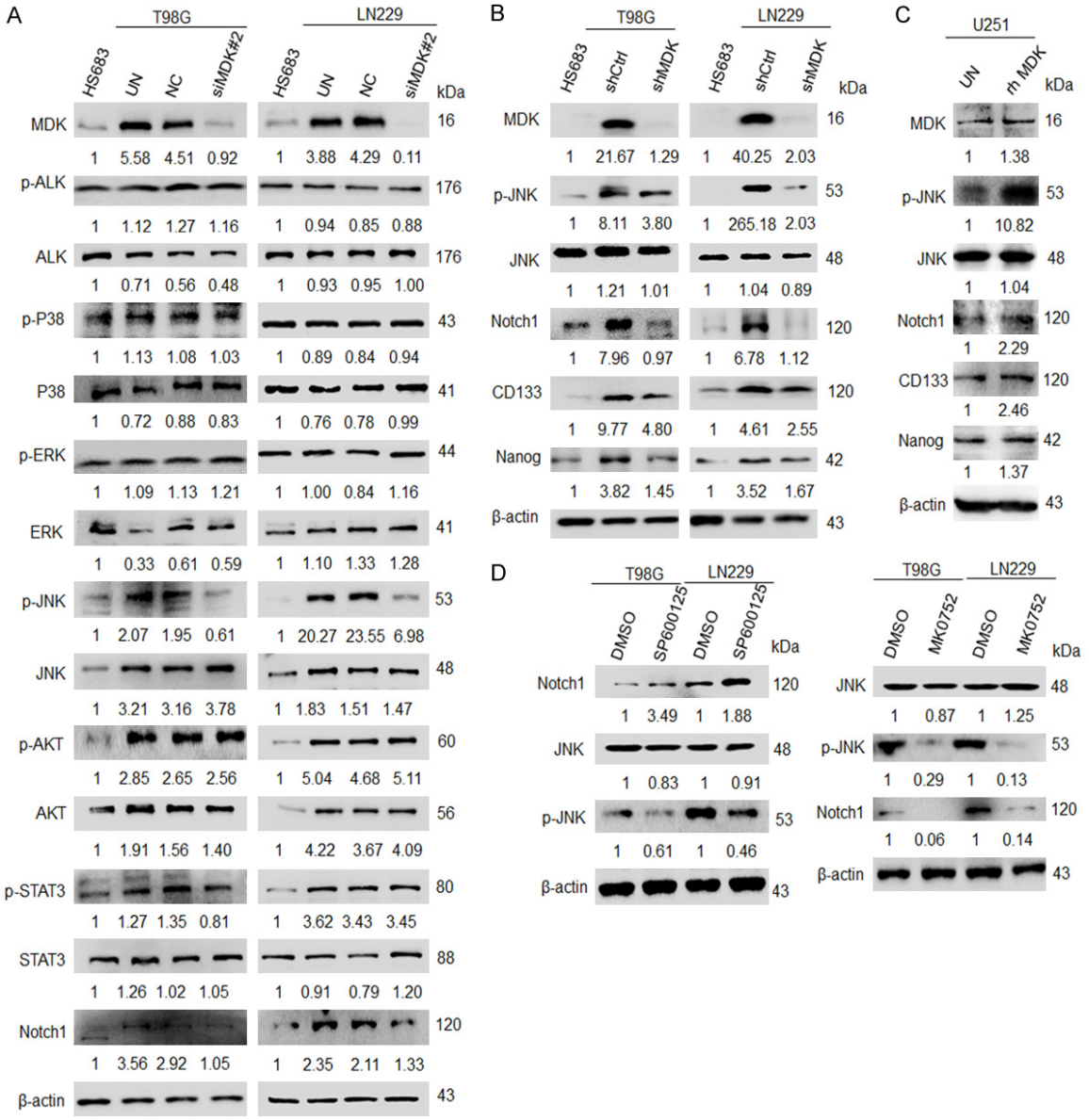

Figure 5. MDK regulates stem-like properties through the Notch1/p-JNK signaling pathway. A. western blot analysis was performed to detect MDK, ALK, P38, ERK, JNK, AKT, STAT3 and Notch1 expression in the siMDK group compared with the control group. B. Western blot analysis was performed to detect MDK, JNK, and Notch1 expression between T98G-shMDK and LN229-shMDK cells and the control group. C. After U251 cells were treated with 0.3 μg/mL rhMDK for 24 h, the expression of MDK, JNK, Notch1, CD133 and Nanog was detected by western blot analysis. D. T98G and LN229 cells were treated with the p-JNK inhibitor SP600125 (10 μM) and Notch1 inhibitor MK-0752 (200 nM) for 24 h, and then western blot analysis was performed to detect the expression of JNK and Notch1. UN: untreated, NC: negative control.

resistance to gemcitabine in biliary tract carcinoma [24]. MDK induces the resistance of glioma cells to tetrahydrocannabinol through the MDK/ALK axis [25]. In the present study, we found that the high expression of MDK in GBM could not only promote proliferation and invasion and inhibit apoptosis but also enhance TMZ resistance in GBM. These results suggested that selectively targeting MDK might be helpful to improve the efficacy of antitumoral therapies for GBM.

To date, various mechanisms, such as DNA repair, autophagy and stemness, have been proven to be involved in the regulation of TMZ resistance [26]. The products from the decom-

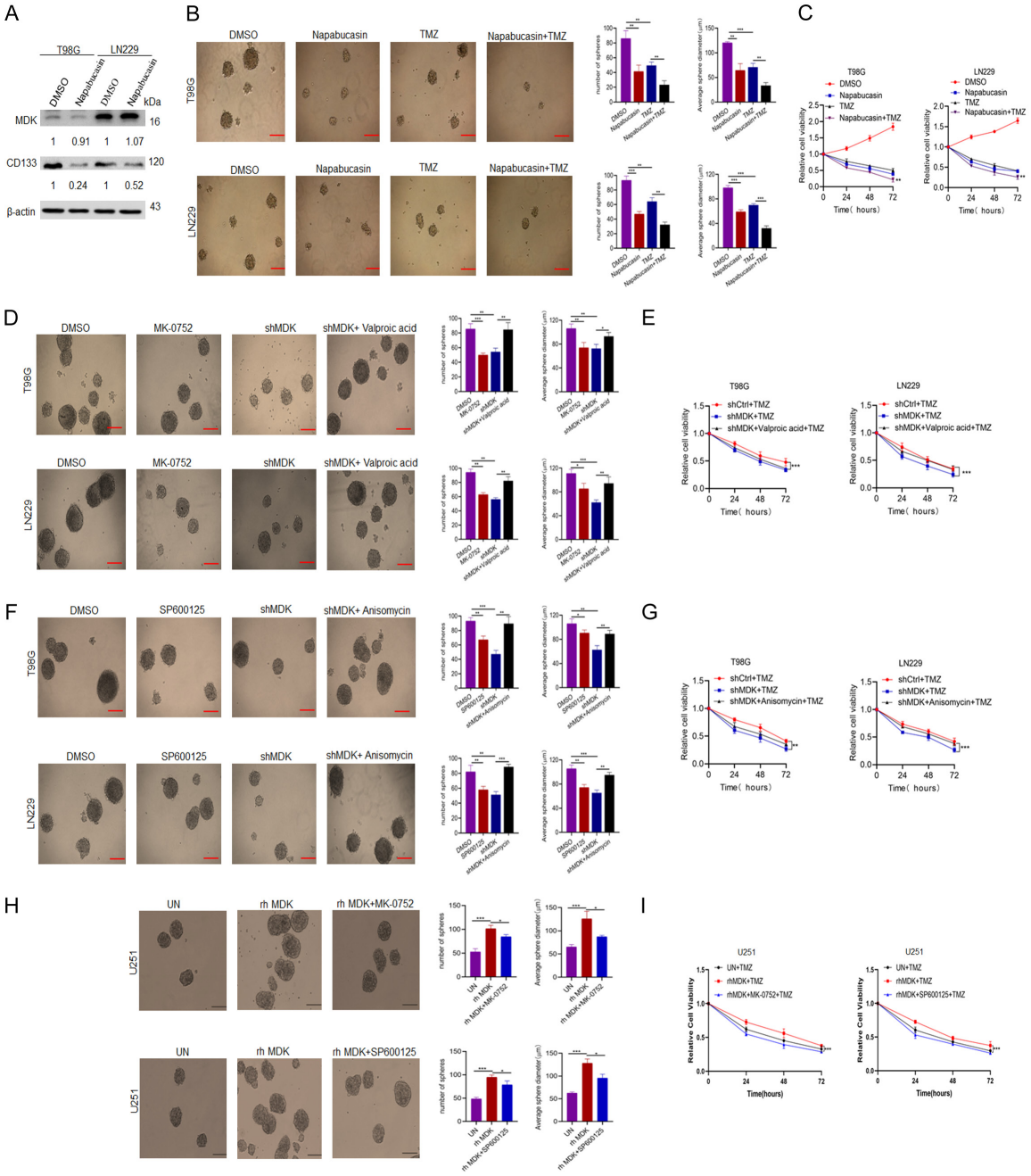

Figure 6. MDK induces TMZ resistance in GBM cells by promoting cancer stem-like properties. A. After T98G and LN229 cells were treated with 0.9 μM and 0.8 μM napabucasin, respectively, western blot assays were used to detect the expression of MDK and CD133. T98G and LN229 cells were treated with 0.9 μM and 0.8 μM napabucasin, respectively, and combined with TMZ treatment (T98G: 700 μM, LN229: 600 μM). B. A sphere formation assay (2 weeks) was performed to detect the stem-like properties of GBM cells. C. Proliferation was detected by the MTS assay. D, F. After treatment with the Notch1 inhibitor MK-0752 (200 nM) or the JNK inhibitor SP600125 (10 μM) in T98G and LN229 cells or treatment with the Notch1 agonist valproic acid (50 μM) or the JNK agonist anisomycin (5 μM) in T98G-shMDK and LN229-shMDK cells, sphere formation was detected (2 weeks). E, G. Valproic acid or anisomycin combined with TMZ treatment in T98G-shMDK and LN229-shMDK cells, proliferation was detected by MTS assay. H. After treatment with 0.3 μg/ml rhMDK and the Notch1 inhibitor MK-0752 (80 nM) or the JNK inhibitor SP600125 (20 μM) in U251 cells, sphere formation was detected (2 weeks). I. After treatment with 0.3 μg/ml rhMDK and the Notch1 inhibitor MK-0752 (80 nM) or the JNK inhibitor SP600125 (20 μM) combined with TMZ treatment in U251 cells, proliferation was detected by MTS assay. Columns: mean of three replicates, **: $p<0.01$, ***: $p<0.001$.

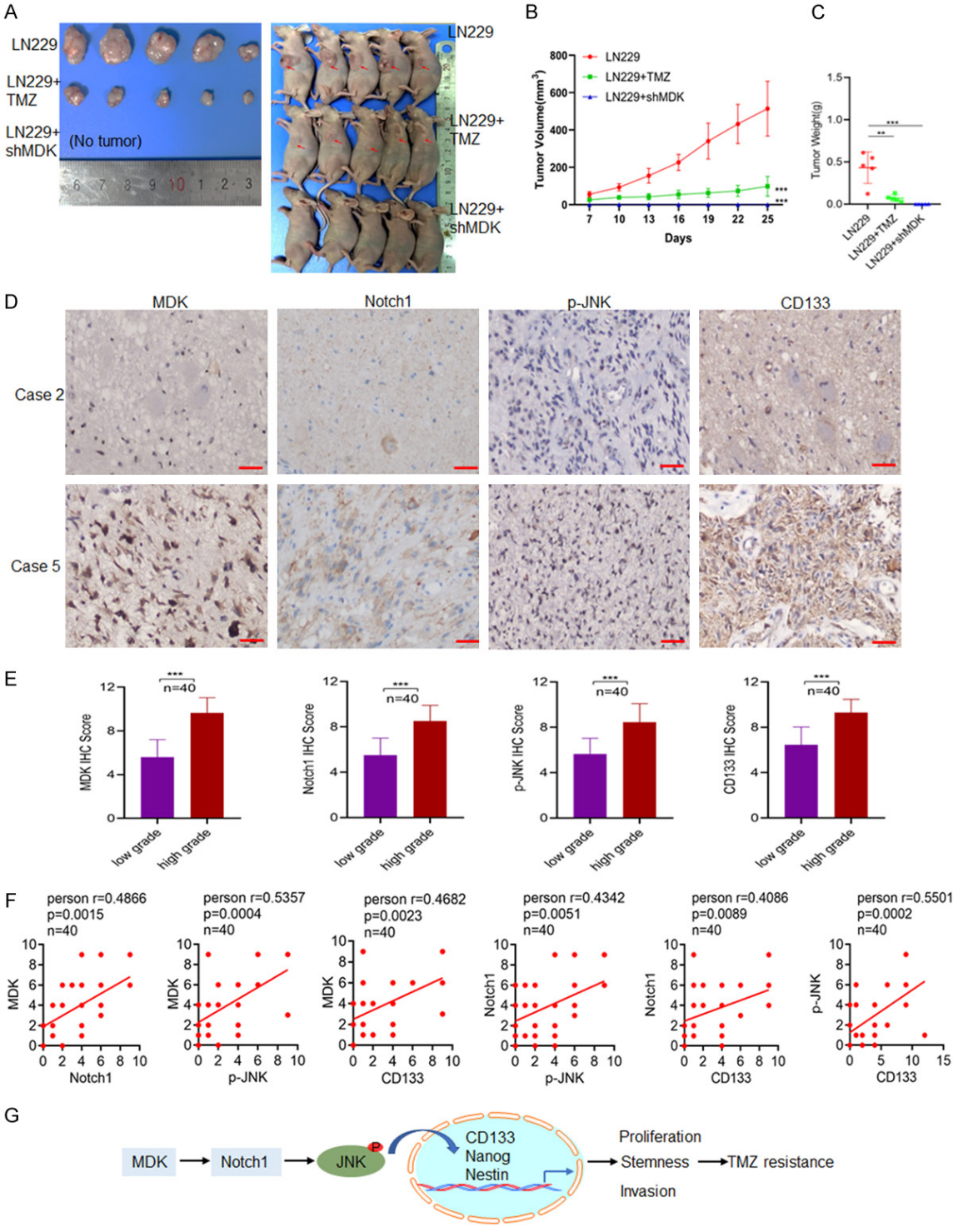

Figure 7. MDK knockdown suppresses GBM growth through the Notch1/p-JNK pathway. LN229 and LN229-shMDK (1×10^7) cells were injected subcutaneously into nude mice, and intraperitoneal injection of TMZ (1 mg/d/20 g, once a day, lasting 4 days, 2 rounds) was administered after the tumor volume reached 60-80 mm^3. A. At the experimental end point, xenografts were dissected and photographed. B. Tumor volume was measured every 3 days. C. Tumor weight was measured at the experimental end point. D. Representative images of IHC staining of tumor tissues from 40 clinical patients. E. The expression differences of MDK, Notch1, p-JNK and CD133 between high- and low-grade gliomas were analyzed from the IHC data. F. The correlations among MDK, Notch1, p-JNK and CD133 were analyzed by Kendall's tau tests. The n (number of independent tissue samples) and *p* value (two sided) are indicated. Scale bar: 100 μm, *: $p<0.05$, ***: $p<0.001$. G. Schematic diagram of MDK's role in regulating stem-like properties through the Notch1/p-JNK signaling pathway and further promoting TMZ resistance in GBM.

position of TMZ into tumor cells can lead to DNA methylation, resulting in DNA damage. However, there is a strong DNA repair system in GBM cells. Tumor cells are repaired by DNA mismatch repair (MMR) and the base excision repair pathway (BER) initiated by DNA glycosylases, such as N-methylpurine DNA glycosylase (APNG), or demethylases, such as O6-methylguanine-DNA-methyltransferase (MGMT), which lead to TMZ resistance in GBM [27, 28]. Cyclopropylamine inhibited the HH/Gli1 signaling pathway and decreased the expression of MGMT, which increased the sensitivity to TMZ in U251 cells [26]. Autophagy is a process in which cells degrade damaged organelles and abnormally folded or dysfunctional proteins through the lysosome pathway. Autophagy can also be used as a cytoprotective mechanism leading to drug resistance of tumor cells. For example, TMZ can induce an increase in autophagy-related ATP in some glioma cells, which is beneficial to the TMZ resistance of tumor cells [29]. LRRC4 is associated with the DEPTOR/mTOR complex, and this interaction results in autophagy inhibition and further restores the sensitivity of GBMs to TMZ [30]. TRPC5-induced autophagy promotes the resistance of glioma cells to TMZ through the CAMMKβ/AMPKα/mTOR pathway [31]. Our findings indicated that MDK significantly promoted the stem-like properties of GBM, increasing TMZ resistance. Meanwhile, MDK could not affect LC3 expression in GBM cells, suggesting that autophagy was not involved in the regulation of TMZ resistance mediated by MDK. Unfortunately, this work did not analyze whether MDK promotes GBM resistance by regulating DNA repair, which needs further research.

It should be noted that in this study, we did not study whether MDK promotes GBM resistance by regulating DNA.

MDK is a growth factor that can activate a series of downstream signal cascades and participate in the regulation of various biological functions [10, 32]. MDK mediates its protective effect in glioma cells through ALK, which can interfere with cannabinoid-induced cell death [25]. The MDK/ALK axis regulates the self-renewal capacity of Glioma Initiating Cells by controlling the autophagic degradation of the transcription factor SOX9 (18). Long-stranded noncoding RNA ZFAS1 induces the ERK/JNK/P38 signaling pathway through the combination of miR-624 and MDK to promote the occurrence and development of hepatocellular carcinoma [22]. In gastric cancer cells, MDK activates both the AKT and ERK1/2 pathways to upregulate the expression of cell cycle-related proteins, thus promoting the survival and growth of tumor cells [33]. This eventually leads to the aggravation of lupus nephritis by activating the nuclear transcription factor NFAT and IL-12/STAT signaling [34]. MDK induces EMT by upregulating the Notch1 signaling pathway in biliary tract cancer [24]. In the present study, we found that MDK mainly promotes p-JNK through Notch1 signaling, thus promoting the stem-like properties of GBM cells, while MDK does not seem to have a significant regulatory effect on other related signaling molecules, which should be a tumor- or cell type-dependent mechanism.

In summary, the overexpression of MDK can promote the malignant phenotype and TMZ resistance of GBM cells by promoting the Notch1/p-JNK signaling axis and further enhancing stem-like properties (**Figure 7G**). This study provides a new candidate target for therapeutic intervention of GBM, especially in TMZ-resistant GBM with high MDK expression.

Acknowledgements

This study was supported by grants from the National Natural Science Foundation of China (Grant Nos. 81974466 and 81672761) and the Fundamental Research Funds for the Central Universities of Central South University (1053320183665).

Disclosure of conflict of interest

None.

Address correspondence to: Lifang Yang and Liangfang Shen, Central South University, Xiangya Road 110, Changsha 410078, Hunan, China. E-mail: yanglifang@csu.edu.cn (LFY); lfshen2008@163.com (LFS)

References

[1] Louis DN, Perry A, Reifenberger G, von Deimling A, Figarella-Branger D, Cavenee WK, Ohgaki H, Wiestler OD, Kleihues P and Ellison DW. The 2016 World Health Organization classification of tumors of the central nervous sys-

tem: a summary. Acta Neuropathol 2016; 131: 803-820.
[2] Nayak L and Reardon DA. High-grade gliomas. Continuum (Minneap Minn) 2017; 23: 1548-1563.
[3] Lee SY. Temozolomide resistance in glioblastoma multiforme. Genes Dis 2016; 3: 198-210.
[4] Tomar MS, Kumar A, Srivastava C and Shrivastava A. Elucidating the mechanisms of temozolomide resistance in gliomas and the strategies to overcome the resistance. Biochim Biophys Acta Rev Cancer 2021; 1876: 188616.
[5] Prasad S, Ramachandran S, Gupta N, Kaushik I and Srivastava SK. Cancer cells stemness: a doorstep to targeted therapy. Biochim Biophys Acta Mol Basis Dis 2020; 1866: 165424.
[6] Ravindran Menon D, Hammerlindl H, Torrano J, Schaider H and Fujita M. Epigenetics and metabolism at the crossroads of stress-induced plasticity, stemness and therapeutic resistance in cancer. Theranostics 2020; 10: 6261-6277.
[7] Tsai YT, Wu AC, Yang WB, Kao TJ, Chuang JY, Chang WC and Hsu TI. ANGPTL4 induces TMZ resistance of glioblastoma by promoting cancer stemness enrichment via the EGFR/AKT/4E-BP1 cascade. Int J Mol Sci 2019; 20: 5625.
[8] Im CN, Yun HH and Lee JH. Heat shock factor 1 depletion sensitizes A172 glioblastoma cells to temozolomide via suppression of cancer stem cell-like properties. Int J Mol Sci 2017; 18: 468.
[9] Wang Z, Yang J, Xu G, Wang W, Liu C, Yang H, Yu Z, Lei Q, Xiao L, Xiong J, Zeng L, Xiang J, Ma J, Li G and Wu M. Targeting miR-381-NEFL axis sensitizes glioblastoma cells to temozolomide by regulating stemness factors and multidrug resistance factors. Oncotarget 2015; 6: 3147-3164.
[10] Filippou PS, Karagiannis GS and Constantinidou A. Midkine (MDK) growth factor: a key player in cancer progression and a promising therapeutic target. Oncogene 2020; 39: 2040-2054.
[11] Hu B, Qin C, Li L, Wei L, Mo X, Fan H, Lei Y, Wei F and Zou D. Midkine promotes glioblastoma progression via PI3K-Akt signaling. Cancer Cell Int 2021; 21: 509.
[12] Hu R, Yan Y, Li Q, Lin Y, Jin W, Li H, Lu Y and Pang T. Increased drug efflux along with midkine gene high expression in childhood B-lineage acute lymphoblastic leukemia cells. Int J Hematol 2010; 92: 105-110.
[13] Kang HC, Kim IJ, Park HW, Jang SG, Ahn SA, Yoon SN, Chang HJ, Yoo BC and Park JG. Regulation of MDK expression in human cancer cells modulates sensitivities to various anticancer drugs: MDK overexpression confers to a multi-drug resistance. Cancer Lett 2007; 247: 40-47.
[14] Han S, Shin H, Lee JK, Liu Z, Rabadan R, Lee J, Shin J, Lee C, Yang H, Kim D, Kim SH, Kim J, Oh JW, Kong DS, Lee JI, Seol HJ, Choi JW, Kang HJ and Nam DH. Secretome analysis of patient-derived GBM tumor spheres identifies midkine as a potent therapeutic target. Exp Mol Med 2019; 51: 1-11.
[15] Lopez-Valero I, Davila D, Gonzalez-Martinez J, Salvador-Tormo N, Lorente M, Saiz-Ladera C, Torres S, Gabicagogeascoa E, Hernandez-Tiedra S, Garcia-Taboada E, Mendiburu-Elicabe M, Rodriguez-Fornes F, Sanchez-Dominguez R, Segovia JC, Sanchez-Gomez P, Matheu A, Sepulveda JM and Velasco G. Midkine signaling maintains the self-renewal and tumorigenic capacity of glioma initiating cells. Theranostics 2020; 10: 5120-5136.
[16] Zhao H, Wang C, Lu B, Zhou Z, Jin Y, Wang Z, Zheng L, Liu K, Luo T, Zhu D, Chi G, Luo Y and Ge P. Pristimerin triggers AIF-dependent programmed necrosis in glioma cells via activation of JNK. Cancer Lett 2016; 374: 136-148.
[17] Lu Z, Miao Y, Muhammad I, Tian E, Hu W, Wang J, Wang B, Li R and Li J. Colistin-induced autophagy and apoptosis involves the JNK-Bcl2-Bax signaling pathway and JNK-p53-ROS positive feedback loop in PC-12 cells. Chem Biol Interact 2017; 277: 62-73.
[18] Yi L, Zhou X, Li T, Liu P, Hai L, Tong L, Ma H, Tao Z, Xie Y, Zhang C, Yu S and Yang X. Notch1 signaling pathway promotes invasion, self-renewal and growth of glioma initiating cells via modulating chemokine system CXCL12/CXCR4. J Exp Clin Cancer Res 2019; 38: 339.
[19] Platta CS, Greenblatt DY, Kunnimalaiyaan M and Chen H. Valproic acid induces Notch1 signaling in small cell lung cancer cells. J Surg Res 2008; 148: 31-37.
[20] Hubbard JM and Grothey A. Napabucasin: an update on the first-in-class cancer stemness inhibitor. Drugs 2017; 77: 1091-1103.
[21] Yang L, Liu L, Xu Z, Liao W, Feng D, Dong X, Xu S, Xiao L, Lu J, Luo X, Tang M, Bode AM, Dong Z, Sun L and Cao Y. EBV-LMP1 targeted DNAzyme enhances radiosensitivity by inhibiting tumor angiogenesis via the JNKs/HIF-1 pathway in nasopharyngeal carcinoma. Oncotarget 2015; 6: 5804-5817.
[22] Duan R, Li C, Wang F, Han F and Zhu L. The long noncoding RNA ZFAS1 potentiates the development of hepatocellular carcinoma via the microRNA-624/MDK/ERK/JNK/P38 signaling pathway. Onco Targets Ther 2020; 13: 4431-4444.
[23] Zhang Y, Deng C, Qian J, Zhang M and Li X. Improvement of radiotherapy-induced lacrimal

gland injury by induced pluripotent stem cell-derived conditioned medium via MDK and inhibition of the p38/JNK pathway. Int J Mol Sci 2014; 15: 18407-18421.
[24] Lu Y, Yan B, Guo H, Qiu L, Sun X, Wang X, Shi Q and Bao Y. Effect of midkine on gemcitabine resistance in biliary tract cancer. Int J Mol Med 2018; 41: 2003-2011.
[25] Lorente M, Torres S, Salazar M, Carracedo A, Hernandez-Tiedra S, Rodriguez-Fornes F, Garcia-Taboada E, Melendez B, Mollejo M, Campos-Martin Y, Lakatosh SA, Barcia J, Guzman M and Velasco G. Stimulation of the midkine/ALK axis renders glioma cells resistant to cannabinoid antitumoral action. Cell Death Differ 2011; 18: 959-973.
[26] Wang K, Chen D, Qian Z, Cui D, Gao L and Lou M. Hedgehog/Gli1 signaling pathway regulates MGMT expression and chemoresistance to temozolomide in human glioblastoma. Cancer Cell Int 2017; 17: 117.
[27] Kaina B and Christmann M. DNA repair in personalized brain cancer therapy with temozolomide and nitrosoureas. DNA Repair (Amst) 2019; 78: 128-141.
[28] Yoshimoto K, Mizoguchi M, Hata N, Murata H, Hatae R, Amano T, Nakamizo A and Sasaki T. Complex DNA repair pathways as possible therapeutic targets to overcome temozolomide resistance in glioblastoma. Front Oncol 2012; 2: 186.
[29] Kanzawa T, Germano IM, Komata T, Ito H, Kondo Y and Kondo S. Role of autophagy in temozolomide-induced cytotoxicity for malignant glioma cells. Cell Death Differ 2004; 11: 448-457.
[30] Feng J, Zhang Y, Ren X, Li D, Fu H, Liu C, Zhou W, Liu Q, Liu Q and Wu M. Leucine-rich repeat containing 4 act as an autophagy inhibitor that restores sensitivity of glioblastoma to temozolomide. Oncogene 2020; 39: 4551-4566.
[31] Zou Y, Chen M, Zhang S, Miao Z, Wang J, Lu X and Zhao X. TRPC5-induced autophagy promotes the TMZ-resistance of glioma cells via the CAMMKbeta/AMPKalpha/mTOR pathway. Oncol Rep 2019; 41: 3413-3423.
[32] Kadomatsu K, Kishida S and Tsubota S. The heparin-binding growth factor midkine: the biological activities and candidate receptors. J Biochem 2013; 153: 511-521.
[33] Xu Y, Qu X, Zhang X, Luo Y, Zhang Y, Luo Y, Hou K and Liu Y. Midkine positively regulates the proliferation of human gastric cancer cells. Cancer Lett 2009; 279: 137-144.
[34] Masuda T, Maeda K, Sato W, Kosugi T, Sato Y, Kojima H, Kato N, Ishimoto T, Tsuboi N, Uchimura K, Yuzawa Y, Maruyama S and Kadomatsu K. Growth factor midkine promotes T-cell activation through nuclear factor of activated T cells signaling and Th1 cell differentiation in lupus nephritis. Am J Pathol 2017; 187: 740-751.

Table S1. Clinical data of pathological specimens of glioma

Case number	Gender	Age	WHO Classification	Types
1	Female	68	IV	Glioblastoma
2	Female	40	IV	Glioblastoma
3	Female	48	IV	Glioblastoma
4	Male	45	IV	Glioblastoma
5	Female	30	IV	Glioblastoma
6	Male	28	II	Diffuse astrocytoma
7	Male	28	II	Diffuse astrocytoma Diffuse astroglioma
8	Male	30	II	Diffuse astrocytoma Diffuse astroglioma
9	Male	42	II	Diffuse astrocytoma Diffuse astroglioma
10	Male	40	II	Diffuse astrocytoma Diffuse astroglioma

Table S2. siMDK target sequence for RNA interference

ID	*target sequence (5'-3')*
GenOFFTM st-h-MDK_001	*CCAAGAAAGGGAAGGGAAA*
GenOFFTM st-h-MDK_002	*GACCAAAGCAAAGGCCAAA*
GenOFFTM st-h-MDK_003	*GCAAGTACAAGTTTGAGAA*

Table S3. shMDK target sequence for RNA interference

ID	*target sequence (5'-3')*
shMDK#1	*TGTCTGCTCGTTAGCTTTAAT*
shMDK#2	CGACTGCAAGTACAAGTTTGA

Table S4. Primers for quantitative RT-PCR

Gene name	*Forward sequence (5' to 3')*	*Reverse sequence (5' to 3')*
MDK	*TTGGAGCCGACTGCAAGTACAAG*	*GGTCTCCTGGCACTGAGCATTG*
CD133	*CACTACCAAGGACAAGGCGTTC*	*CAACGCCTCTTTGGTCTCCTTG*
NANOG	*CCCCAGCCTTTACTCTTCCTA*	*CCAGGTTGAATTGTTCCAGGTC*
β-Actin	*CATGTACGTTGCTATCCAGGC*	*CTCCTTAATGTCACGCACGAT*

Table S5. Clinical characteristics of glioma patients

Characteristics	No. of patients(%)
Gender	
Male	25 (62.5)
Female	15 (37.5)
Age(years)	
<40	20 (50.0)
≥40	20 (50.0)
WHO Classification	
I	5 (12.5)
II	10 (25.0)
III	8 (20.0)
IV	17 (42.5)
Tumor resection	
Total	40
Subtotal	0
TMZ	
Yes	16 (40.0)
No	24 (60.0)
Radiotherapy	
Yes	14 (35.0)
No	26 (65.0)
IDH1/2 status	
WT	19 (47.5)
Mutated	13 (32.5)
Unknown	8 (20)

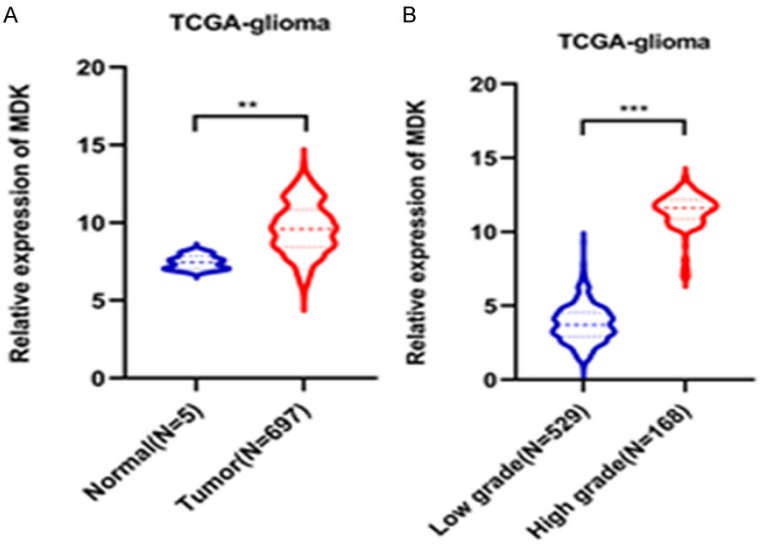

Figure S1. A. The differences in MDK expression between normal glial tissues and glioma tissues were analyzed based on the TCGA database. B. The differences in MDK expression between low-grade glioma tissues and high-grade glioma tissues were analyzed based on the TCGA database.

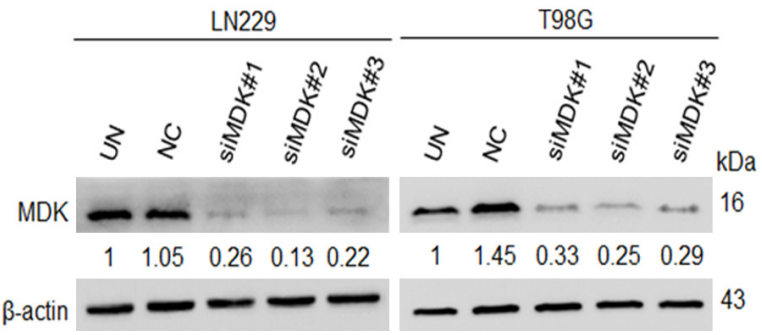

Figure S2. Analysis of the effect of targeting MDK siRNA in GBM cells. LN229 and T98G cells were respectively transfected with three MDK siRNAs for 48 h, and the expression of MDK was analyzed by western blot. UN: untreatment; NC: negative control.

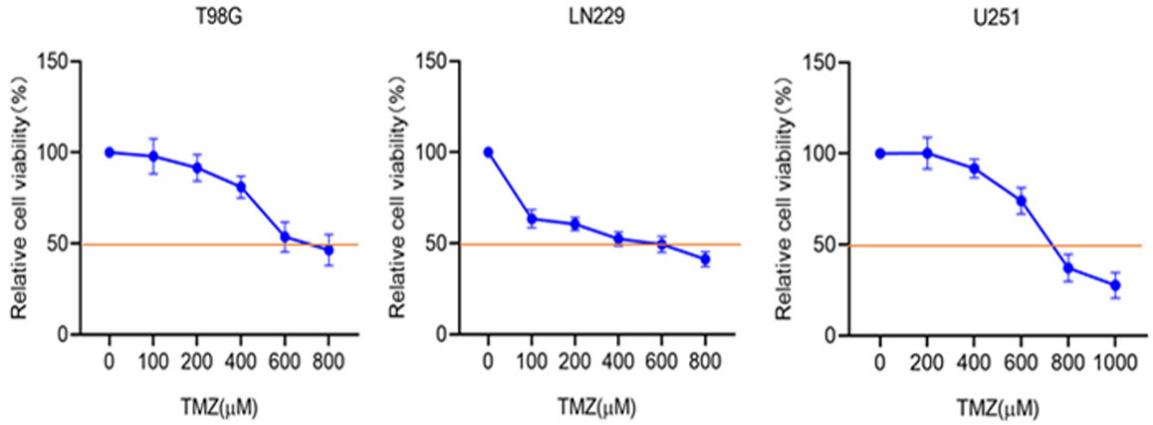

Figure S3. Cell viability of GBM cells at different doses of TMZ after 48 hours of treatment was analyzed by MTS assay. Data, expressed as percent cell viability relative to untreated cells from 3 independent experiments carried out in triplicate, are presented as mean ± SEM in dose-response curves. IC50 values were obtained with GraphPad Prism 8.0.

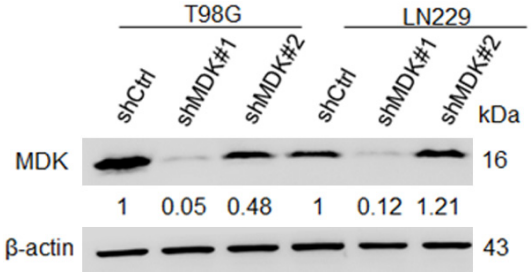

Figure S4. MDK expression was analyzed of T98G-shMDK and LN229-shMDK cells by western blot.

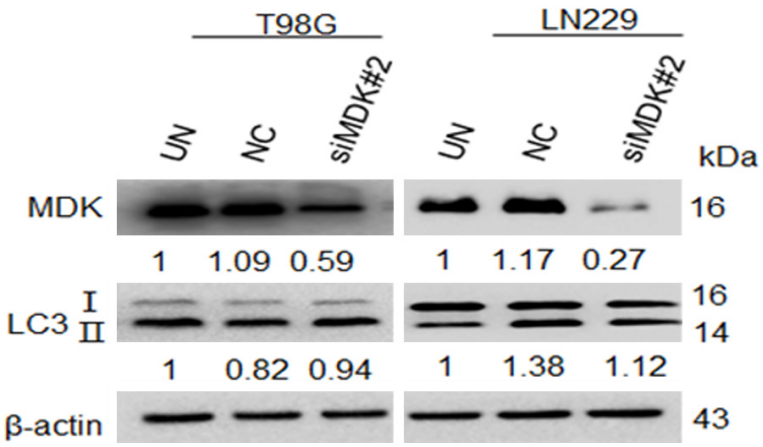

Figure S5. Analysis of the effect of MDK on autophagy in GBM cells. LN229 and T98G cells were transfected with MDK siRNA for 24 h, and the expression of MDK and LC3 I/II were analyzed by western blot. UN: untreatment; NC: negative control.

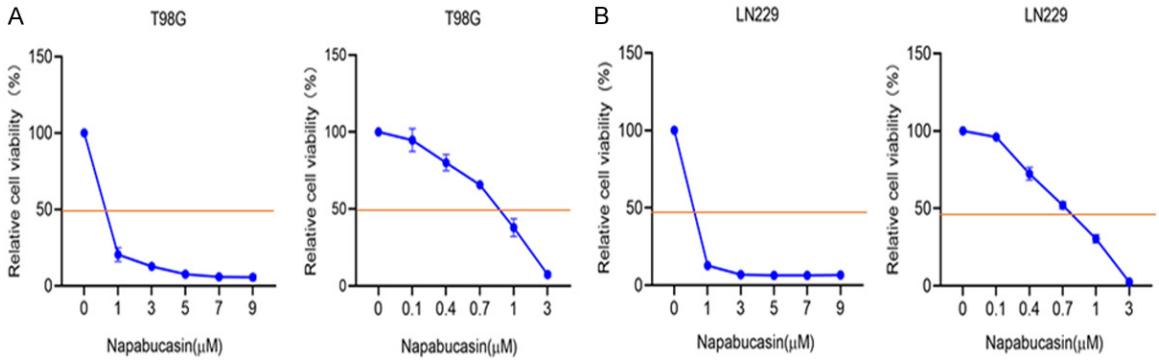

Figure S6. Cell viability of GBM cells at different doses of Napabucasin after 48 hours of treatment were analyzed by MTS assay. (A) T98G cells, (B) LN229 cells data, expressed as percent cell viability relative to untreated cells from 3 independent experiments carried out in triplicate, are presented as mean ± SEM in dose-response curves. IC50 values were obtained with GraphPad Prism 8.0.

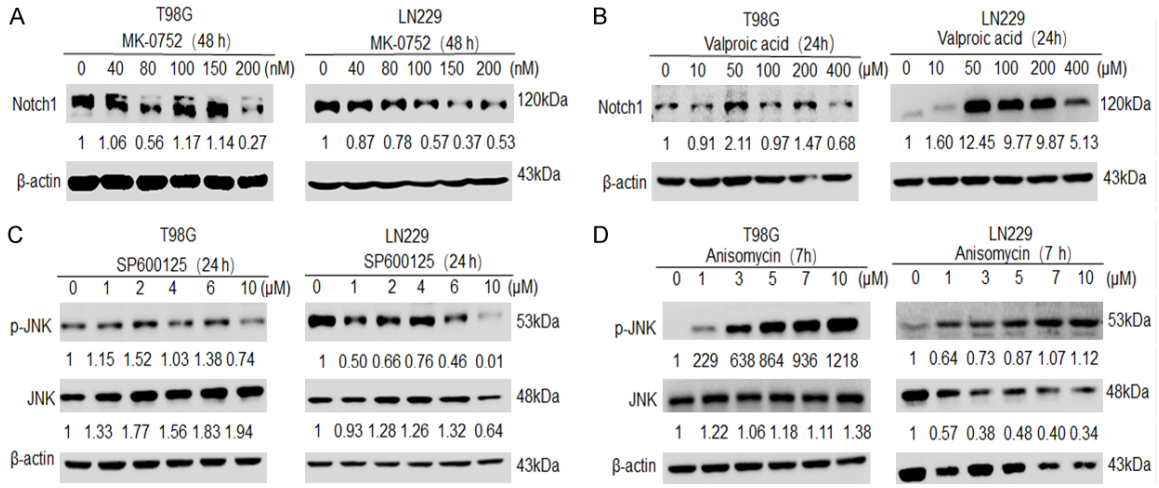

Figure S7. For screening of optimal working concentration of (A) Notch1 inhibitor MK-0752, (B) Notch1 agonist valproic acid, (C) p-JNK inhibitor SP600125, (D) P-JNK agonist Anisomycin, were analyzed in T98G and LN229 cells by Western blot.